NIST Reference Densitometer for Visual Diffuse Transmission Density

Edward A. Early, Christopher L. Cromer, Xiaoxiong Xiong, Daniel J. Dummer, Thomas R. O'Brian, and Albert C. Parr

Optical Technology Division, National Institute of Standards and Technology, Gaithersburg, Maryland

The Optical Technology Division of the National Institute of Standards and Technology has developed a new reference densitometer for measuring visual diffuse transmission densities using the diffuse influx mode. This densitometer is used to calibrate both x-ray and photographic film step tablet Standard Reference Materials. The design, characterization, and operation of the densitometer are detailed. The densitometer was fully characterized both to verify compliance with the applicable documentary standards and to determine the combined uncertainty in transmission density associated with the calibrations.

Journal of Imaging Science and Technology 43: 388–397 (1999)

Visual diffuse transmission density is an important physical property for exposed films, and therefore has great industrial demand for process control in the fields of medicine, non-destructive testing, photography, and graphic arts. Standards for visual diffuse transmission density are provided by the National Institute of Standards and Technology (NIST) in the form of Standard Reference Materials (SRMs). These standards are film step tablets, 254 mm long by 35 mm wide, with steps extending the width of each film and equally spaced along its length. A double emulsion x-ray film is used for SRM 1001, while a single emulsion photographic film is used for SRM 1008. The steps have increasing visual diffuse transmission densities from approximately 0.1 to 4 from one end of the film to the other. SRM 1001 has 17 steps, while SRM 1008 has 23 steps.

The visual diffuse transmission densities of film step tablets for both SRMs are determined with a new reference densitometer using the diffuse influx mode. Diffuse illumination is achieved with a lamp, filter, and flash opal, while directional detection is accomplished with a lens, filter, and photodiode system. The densitometer is designed to automatically measure many films using computerized data acquisition and control.

This article states the relevant measurement equations for determining visual diffuse transmission density, describes the densitometer's design and operation, and details the characterization of the densitometer and the resulting uncertainties in the measurement. Additional details can be found in Ref. 1.

Measurement Equations

The purpose of the measurement equation derived in this section is to obtain a mathematical description of the measurement of visual diffuse transmission density. This is useful for calculating the transmission density from the experimental results, for determining the uncertainty in these values, and for relating measurements made with the densitometer to those that would be made by an ideal densitometer—one that exactly conforms to all the relevant documentary standards.

As specified in the documentary standards,[2–4] visual diffuse transmission density is essentially a photopic transmission measurement using a hemispherical/directional geometry, with the added complication that the transmission is determined with the sample in contact with an opal. Therefore, the nomenclature and equations from photometry and spectrophotometry will be used as much as possible to derive the measurement equation.

Following the nomenclature given in Refs. 2 and 5, visual diffuse transmission density is determined from two luminous fluxes, the aperture flux Φ_j and the transmitted flux Φ_τ. The first is the flux emerging from the sampling aperture in the directions and parts of the spectrum used in the measurement; the second is the flux that passes through the sample, emerging from a surface other than that on which the incident flux falls, and then used in the measurement. In terms of these fluxes, the visual diffuse transmittance factor T_v is given by

$$T_V = \frac{\Phi_\tau}{\Phi_j} \tag{1}$$

and the visual diffuse transmission density D_T is defined by

$$D_T = -\log_{10} T_V. \tag{2}$$

To this point, neither the spatial nor spectral properties of the fluxes have been specified. For the spatial properties, some nomenclature must first be defined. The incident flux is referred to as the influx, while the transmitted flux is referred to as the efflux. These fluxes can either be hemispherical (in all directions) or directional (in one specified direction). For visual *diffuse* transmission density, there are two possible equivalent measurement geometries, with equivalence being as-

Original manuscript received December 7, 1998

sumed by the Helmholtz reciprocity theorem.[6] In the diffuse influx mode the influx is diffuse and detection of the efflux is directional; in the diffuse efflux mode the influx is directional and detection of the efflux is diffuse.[3] Using the terminology from spectrophotometry, these geometries are hemispherical/directional and directional/hemispherical, respectively.

For *visual* diffuse transmission density, the spectral product of the influx and the detector are specified[4] so that the integral is a luminous flux. In general, luminous flux Φ_v [lm] is defined as

$$\Phi_V = K_m \cdot \int d\lambda\, S(\lambda) \cdot V_\lambda(\lambda), \quad (3)$$

where K_m = 683 lm/W is the maximum spectral luminous efficacy for photopic vision, λ [nm] is the wavelength, $S(\lambda)$ [W/nm] is the spectral flux distribution, and $V_\lambda(\lambda)$ is the spectral luminous efficiency function. For visual diffuse transmission density, the spectral flux distribution of the incident flux is denoted by $S_H(\lambda)$ and the relative spectral response function $V(\lambda)$ of the detection system is denoted by $V_T(\lambda)$. Note that $V(\lambda)$ is a normalized, unitless function, as is $V_\lambda(\lambda)$. $S_H(\lambda)$ is based on the spectral flux distribution of CIE Standard Illuminant A, $S_A(\lambda)$, modified at infrared wavelengths to protect the sample and optical elements from excessive heat, and $V_T(\lambda)$ is defined so that

$$S_H(\lambda) \cdot V_T(\lambda) = S_A(\lambda) \cdot V_\lambda(\lambda). \quad (4)$$

Therefore, because the spectral product on the right-hand-side of Eq. 4 is the same as that integrated in Eq. 3, visual diffuse transmission density is determined from luminous fluxes.

In terms of the definitions and concepts presented in the previous paragraph, the densitometer measures visual diffuse transmission density using the diffuse influx mode. The important components of the densitometer are shown in Fig. 1, as well as a spherical coordinate system. The film step tablet is in contact with the opal that provides an influx with a hemispherical geometry and a spectral flux distribution $S_H(\lambda)$. The efflux is collected within an acceptance cone at normal incidence to the film surface and having a half-angle κ less than 10°, and with a relative spectral response function $V_T(\lambda)$. The aperture stop of the optical system is the collecting lens, while the opal is the aperture that defines the aperture flux. Using the functional notation specified in Refs. 2, 3, and 5, the measured visual diffuse transmission density is described by

$$D_T(90° \text{ opal}; S_H :\leq 10°; V_T). \quad (5)$$

The aperture flux Φ_j measured by the densitometer is given by

$$\Phi_j = K_m \cdot \int dA_j \int d\Omega_j \int d\lambda\, L_j(A_j, \theta_j, \phi_j; \lambda) \cdot V(\lambda) = \frac{I_j}{R_j}, \quad (6)$$

where A_j [m²] is the area over which the aperture flux emerges, Ω_j [sr] is the projected solid angle over which the aperture flux is collected, θ_j and ϕ_j are the polar and azimuth angle, respectively, of the aperture flux, L_j [W/(m² sr nm)] is the aperture spectral radiance from the opal, I_j [A] is the current from the photodiode for the aperture flux, and R_j [A/lm] is the photometric responsivity of the detector. For a Lambertian spectral radiance, the integrals over A_j and Ω_j yield the throughput of the densitometer. An immediate simplifying assumption for Eq. 6 is that the spectral radiance L_j is

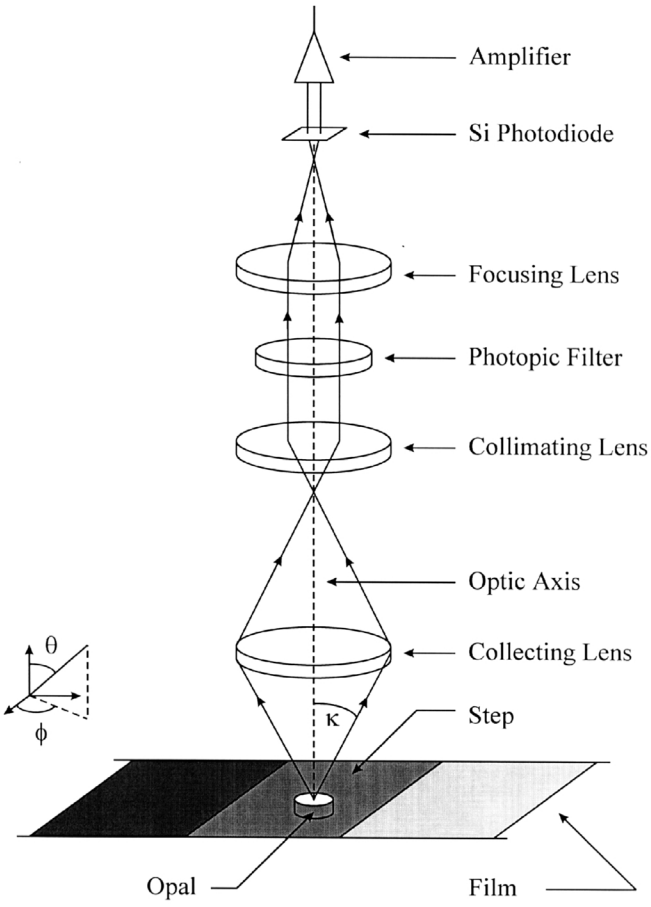

Figure 1. Schematic diagram of the important components of the visual diffuse transmission densitometer.

uniform over the area A_j, and that A_j is small enough so that Ω_j is the same at all points of this area. This is reasonable because the flux from the opal varies by less than 8% from its value at the center and the opal is much smaller than the aperture stop of the detection system. Then, Eq. 6 becomes

$$\Phi_j = K_m \cdot A_j \cdot \int d\Omega_j \int d\lambda\, L_j(A_j, \theta_j, \phi_j; \lambda) \cdot V(\lambda) = \frac{I_j}{R_j}. \quad (7)$$

Similarly, the transmitted flux Φ_τ measured by the densitometer is given by

$$\Omega_\tau = K_m \cdot A_\tau \cdot \int d\Omega_\tau \int d\lambda\, L_\tau(\theta_\tau, \phi_\tau; \lambda) \cdot V(\lambda) = \frac{I_\tau}{R_\tau}, \quad (8)$$

where A_τ [m²] is the area over which the transmitted flux emerges, Ω_τ [sr] is the projected solid angle over which the transmitted flux is collected, θ_τ and ϕ_τ are the polar and azimuth angle, respectively, of the transmitted flux, L_τ [W/(m² sr nm)] is the transmitted spectral radiance from the sample, I_τ [A] is the current from the photodiode from the transmitted flux, and R_τ [A/lm] is the photometric responsivity of the detector. The transimpedance amplifier with gain G [V/A] converts the current from the photodiode to a voltage signal N [V] for both fluxes.

The sample has a spectral hemispherical/directional transmittance $\tau(2\pi; \theta_\tau, \phi_\tau; \lambda)$, where 2π indicates that the incident flux is over the entire hemisphere. This transmittance is related to the bi-directional transmittance distribution function (BTDF) $f_t(\theta_i, \phi_i; \theta_\tau, \phi_\tau; \lambda)$ [sr⁻¹] by

$$\tau(2\pi;\theta_\tau,\phi_\tau;\lambda)=\frac{1}{\pi}\cdot\int f_t(\theta_i,\phi_i;\theta_\tau,\phi_\tau;\lambda)\,d\Omega_i\,, \qquad (9)$$

where the integral of the projected solid angle is over the entire hemisphere. Note that the BTDF is the transmittance analog of BRDF, and relates the incident irradiance to the transmitted radiance. As specified in the documentary standards, the sample is in contact with the opal,[3] and therefore the radiant flux transmitted by the sample also includes flux from the inter-reflections between the sample and the opal. This situation is described by the spectral hemispherical/directional transmittance factor $T(2\pi;\ \theta_\tau,\ \phi_\tau;\ \lambda)$, that depends on both the spatial and spectral variables and is given by

$$T(2\pi;\theta_\tau,\phi_\tau;\lambda)=\frac{\tau(2\pi;\theta_\tau,\phi_\tau;\lambda)}{1-\rho_o(2\pi;\theta_\tau,\phi_\tau;\lambda)\cdot\rho(2\pi;\theta_\tau,\phi_\tau;\lambda)}. \qquad (10)$$

The spectral hemispherical/directional reflectance of the opal and sample are $\rho_o(2\pi;\ \theta_\tau,\ \phi_\tau;\ \lambda)$ and $\rho(2\pi;\ \theta_\tau,\ \phi_\tau;\ \lambda)$, respectively. Thus, the transmitted spectral radiance L_τ is

$$L_\tau(\theta_\tau,\phi_\tau;\lambda)=L_j(2\pi;\lambda)\cdot T(2\pi;\theta_\tau,\phi_\tau;\lambda)\,, \qquad (11)$$

where $L_j(2\pi;\ \lambda)$ is the spectral radiance incident on the sample from the entire hemisphere. As with transmittance, the spectral hemispherical/directional transmittance factor is related to the bi-directional transmittance factor distribution function (BTFDF) $f_T(\theta_i,\ \phi_i;\ \theta_\tau,\ \phi_\tau;\ \lambda)$ [sr^{-1}] by

$$T(2\pi;\theta_\tau,\phi_\tau;\lambda)=\frac{1}{\pi}\cdot\int f_T(\theta_i,\phi_i;\theta_\tau,\phi_\tau;\lambda)\,d\Omega_i\,. \qquad (12)$$

Combining Eqs. 7, 8, and 11, the visual diffuse transmittance factor T_v measured by the densitometer is given by

$$T_v=\frac{\Phi_\tau}{\Phi_j}=\frac{A_\tau\cdot\int d\Omega_\tau\int d\lambda\,L_j(2\pi;\lambda)\cdot T(2\pi;\theta_\tau,\phi_\tau;\lambda)\cdot V(\lambda)}{A_j\cdot\int d\Omega_j\int d\lambda\,L_j(\theta_j,\phi_j;\lambda)\cdot V(\lambda)}=\frac{N_\tau}{N_j}\cdot\frac{G_j}{G_\tau}\cdot\frac{R_j}{R_\tau}. \qquad (13)$$

The analysis is simplified by assuming that the spatial and spectral variables can be separated in Eq. 13, which is equivalent to assuming that the spatial properties of T and L_j are independent of wavelength. Therefore, Eq. 13 becomes

$$T_v=\frac{A_\tau}{A_j}\cdot\frac{\int d\Omega_\tau\,l_j(2\pi)\cdot T(2\pi;\theta_\tau,\phi_\tau)}{\int d\Omega_j\,l_j(\theta_j,\phi_j)}\cdot\frac{\int d\lambda\,S(\lambda)\cdot T(\lambda)\cdot V(\lambda)}{\int d\lambda\,S(\lambda)\cdot V(\lambda)}, \qquad (14)$$

where $l_j(2\pi)$ and $l_j(\theta_j,\ \phi_j)$ [$1/(m^2\ sr)$] are the relative spatial radiance distributions over the entire hemisphere and within the acceptance cone, respectively, $T(2\pi;\ \theta_\tau,\ \phi_\tau)$ is the spatial transmittance factor, and $T(\lambda)$ is the spectral transmittance factor.

For the ideal densitometer, the relative spatial radiance distribution $l_j(\theta_i,\ \phi_i)$ is constant for all angles, the spectral flux distribution is $S_A(\lambda)$, and the relative spectral response function is $V_\lambda(\lambda)$. The ideal visual diffuse transmittance function $T_{v,id}$ is then given by

$$T_{v,id}=\frac{A_\tau}{A_j}\cdot\frac{\int d\Omega_\tau\,T(2\pi;\theta_\tau,\phi_\tau)}{\int d\Omega_j}\cdot\frac{\int d\lambda\,S_A(\lambda)\cdot T_o(\lambda)\cdot V_\lambda(\lambda)}{\int d\lambda\,S_A(\lambda)\cdot V_\lambda(\lambda)}, \qquad (15)$$

where $T_o(\lambda)$ is the spectral transmittance factor for an opal with a reflectance specified in the documentary standards. The spatial and spectral terms of Eqs. 14 and 15 are given by the first two fractions and the last fraction, respectively. For the spectral term, the spectral correction factor C_s is given by

$$C_s=\frac{T_{v,id}}{T_v}=\frac{\int d\lambda\,S_A(\lambda)\cdot T_o(\lambda)\cdot V_\lambda(\lambda)}{\int d\lambda\,S(\lambda)\cdot T(\lambda)\cdot V(\lambda)}\cdot\frac{\int d\lambda\,S(\lambda)\cdot V(\lambda)}{\int d\lambda\,S_A(\lambda)\cdot V_\lambda(\lambda)}. \qquad (16)$$

For the spatial terms, the geometrical correction factor C_g is given by

$$C_g=\frac{T_{v,id}}{T_v}=\frac{\int d\Omega_\tau\,T(2\pi;\theta_\tau,\phi_\tau)}{\int d\Omega_\tau\,l_j(2\pi)\cdot T(2\pi;\theta_\tau,\phi_\tau)}\cdot\frac{\int d\Omega_j\,l_j(\theta_j,\phi_j)}{\int d\Omega_j}, \qquad (17)$$

which in terms of the BTFDF from Eq. 12, is

$$C_g=\frac{\int d\Omega_\tau\int d\Omega_i\,f_T(\theta_i,\phi_i;\theta_\tau,\phi_\tau)}{\int d\Omega_\tau\int d\Omega_i\,l_j(\theta_i,\phi_i)\cdot f_T(\theta_i,\phi_i;\theta_\tau,\phi_\tau)}\cdot\frac{\int d\Omega_j\,l_j(\theta_j,\phi_j)}{\int d\Omega_j}. \qquad (18)$$

Therefore, C_g depends on both the relative spatial radiance distribution of the incident radiant flux and on the transmitting properties of the sample.

Consider two extreme examples. First, assume that the sample does not scatter the incident flux, but simply absorbs it. Then, f_T is given by

$$f_T=2\cdot T(\lambda)\cdot\delta(\sin^2\theta_\tau-\sin^2\theta_i)\cdot\delta(\phi_\tau-\pi\pm\phi_i)\,, \qquad (19)$$

where $\delta(x)$ is the Dirac delta-function. Performing the integrals over $d\Omega_i$ with this expression for f_T, Eq. 18 becomes

$$C_g=\frac{\int d\Omega_\tau}{\int d\Omega_\tau\ l_j(\theta_\tau,\phi_\tau)}\cdot\frac{\int d\Omega_j\,l_j(\theta_j,\phi_j)}{\int d\Omega_j}, \qquad (20)$$

which, for the reasonable assumption that the acceptance cones for the aperture and transmitted fluxes are the same, becomes $C_g = 1$. Second, assume that the sample is a Lambertian diffuser, so that $f_T = 1/\pi$. Then, C_g becomes

$$C_g=\frac{\int d\Omega_i}{\int d\Omega_i\ l_j(\theta_i,\phi_i)}\cdot\frac{\int d\Omega_j\,l_j(\theta_j,\phi_j)}{\int d\Omega_j}, \qquad (21)$$

where, assuming that the relative spatial radiance distribution is Lambertian within the acceptance cone, reduces to

$$C_g=\frac{\int d\Omega_i}{\int d\Omega_i\ l_j(\theta_i,\phi_i)}=\frac{1}{d}, \qquad (22)$$

where d is the diffusion coefficient for the opal. From these two extreme cases, the range of C_g is $1 \le C_g \le 1/d$.

Finally, the visual diffuse transmittance of the sample measured with an ideal densitometer, $\tau_{v,id}$, is given by

$$\tau_{v,id}=\frac{\int d\lambda\,S_A(\lambda)\cdot\tau(\lambda)\cdot V_\lambda(\lambda)}{\int d\lambda\,S_A(\lambda)\cdot V_\lambda(\lambda)}, \qquad (23)$$

where $\tau(\lambda)$ is the spectral transmittance of the sample. The transmittance correction factor C_t is then given by

$$C_t = \frac{\tau_{v,id}}{T_{v,id}} = \frac{\int d\lambda\, S_A(\lambda)\cdot\tau(\lambda)\cdot V_\lambda(\lambda)}{\int d\lambda\, S_A(\lambda)\cdot T(\lambda)\cdot V_\lambda(\lambda)}. \quad (24)$$

Combining, Eqs. 13, 16, and 17, the visual diffuse transmittance factor of a sample measured on an ideal densitometer in terms of the measurements and characteristics of the actual densitometer is given by

$$\begin{aligned} T_{v,id} &= T_V \cdot C_S \cdot C_g \\ &= \frac{N_\tau}{N_j}\cdot\frac{G_j}{G_\tau}\cdot\frac{R_j}{R_\tau}\cdot C_S \cdot C_g \end{aligned} \quad (25)$$

and, including Eq. 24, the visual diffuse transmittance of a sample measured by an ideal densitometer without an opal in contact with the sample is given by

$$\begin{aligned} \tau_{v,id} &= T_{v,id}\cdot C_t \\ &= \frac{N_\tau}{N_j}\cdot\frac{G_j}{G_\tau}\cdot\frac{R_j}{R_\tau}\cdot C_S \cdot C_g \cdot C_t. \end{aligned} \quad (26)$$

Note that because all three correction factors are ratios, only relative values of the integrated quantities are needed.

By combining Eqs. 2 and 13, the visual diffuse transmission density measured by the densitometer is given by

$$D_T = -\log_{10} T_V = \log_{10}\left(\frac{\Phi_j}{\Phi_\tau}\right) = \log_{10}\left(\frac{N_j}{N_\tau}\cdot\frac{G_\tau}{G_j}\cdot\frac{R_\tau}{R_j}\right), \quad (27)$$

which is used both to calculate D_T from the experimental values and to determine the uncertainty in D_T from the uncertainties in the variables. By combining Eqs. 25 and 27, the visual diffuse transmission density for an ideal densitometer $D_{T,id}$ is given by

$$D_{T,id} = D_T - \log_{10}(C_S) - \log_{10}(C_g), \quad (28)$$

which is also used to calculate the uncertainty in D_T due to the non-ideal characteristics of the actual densitometer. Finally, the visual diffuse transmittance density for an ideal densitometer without an opal, from Eqs. 25 to 28, is given by

$$D_{\tau,id} = D_T - \log_{10}(C_S) - \log_{10}(C_g) - \log_{10}(C_t). \quad (29)$$

For convenience, visual diffuse transmission density will often be referred to simply as transmission density for the remainder of the paper.

Description and Operation of the Densitometer

The densitometer was designed and built to automatically measure the visual diffuse transmission density of each step of film step tablets using computerized data acquisition and control. A side view of the mechanical, optical, and electrical components of the densitometer, as well as the connections between them and the optical path from the lamp housing to the detector, is shown in Fig. 2. The densitometer is conveniently divided into three systems: source, film transport, and detector.

The source system provides diffuse illumination to the film step tablet with spectral flux distribution $S(\lambda)$, using a lamp and housing, an infrared filter assembly, a shutter, and an opal. A 100 W quartz-tungsten-halogen lamp is contained in the lamp housing and operated at a constant dc current from the lamp power supply. An elliptical reflector focuses the light from this lamp at approximately the position of the opal. The infrared filter consists of a flow of chilled water between two glass plates; the top optical filter is chosen so that the transmittance of the infrared filter modifies the spectral flux distribution from the lamp to one closely approximating $S_H(\lambda)$. The lamp housing is also cooled with chilled water, and if the flow of water is interrupted, the flow meter disables the power supply, preventing the infrared filter from overheating. An electronically controlled shutter blocks all light from reaching the opal for a measurement of the dark signal. A flash opal with a diameter of 3 mm and a thickness of 1.5 mm is the source of diffuse illumination. The opal is mounted in a sleeve and the top is centered in and flush with the vacuum plate described below. Black enamel paint is applied to the sides of the opal so that all the influx originates from the top of the opal, which defines the sampling aperture.

The film transport system picks up film from a tray using a holder, positions the film to measure the transmission density of each step, and drops the film in another tray. A top view of this system is shown in Fig. 3. The film holder is attached to a vertical spring-loaded stage on a vertical translation stage, that in turn is attached to a horizontal translation stage. The film holder and translation stages move the film to the appropriate locations. A vacuum holds the film on the holder and brings the film into direct contact with the opal. The vacuum is applied through solenoids, and an additional solenoid brings air into the holder when the film is dropped in the tray. The film holder has a groove along its outer edge, so that when the holder is in contact with a film and vacuum is applied to this groove, the film is attached to the holder and can be moved. When a film is on the vacuum plate and a vacuum is applied, small holes in the vacuum plate pull the film down onto the opal.

The detector system collects and detects the radiant flux from the opal or the step. The lenses collect the flux within the acceptance cone, collimate it through a photopic filter, and focus it onto a Si photodiode detector. A transimpedance amplifier converts the current from the photodiode to a voltage, that is then measured with a digital voltmeter. A baffle with a diameter of 10 mm reduces scattered light in the detector system. The spectral transmittance of the photopic filter is such that, in combination with the spectral responsivity of the photodiode, the spectral response function of the detector system closely approximates $V_\lambda(\lambda)$. The photopic filter is slightly tilted so that the light reflected from it does not travel back down to the opal. The 4 mm by 4 mm Si photodiode is contained in a package that provides thermoelectric temperature control and transimpedance amplification with a gain that can be selected either manually or automatically. The aperture stop of the optical system is the collecting lens that defines an acceptance cone with a half-angle $\kappa = 9.5°$. If the opal is included in the optical system, it is the field stop; if it is not, the photodiode is the field stop. With this second choice for defining the field stop, the field of view has a

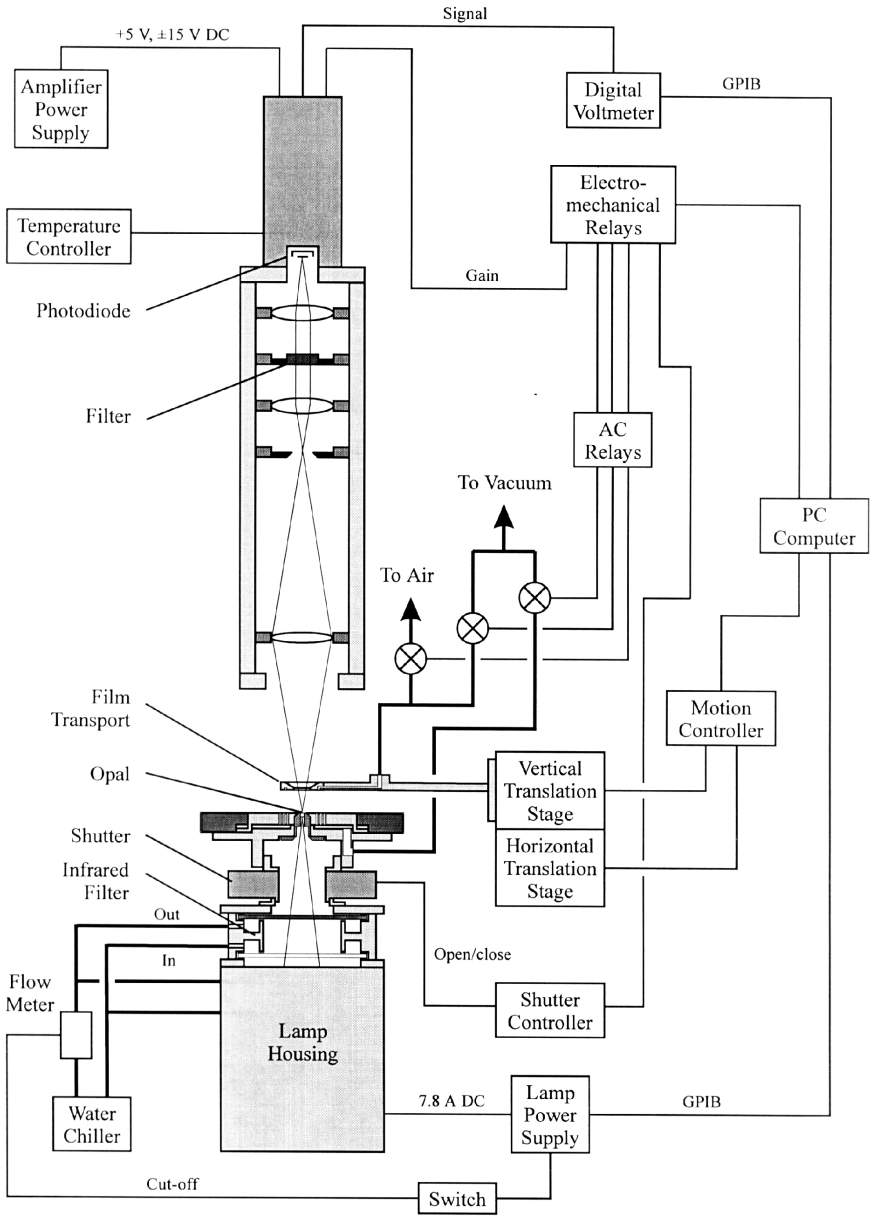

Figure 2. Schematic diagram of all the components of the visual diffuse transmission densitometer and their electrical and mechanical connections.

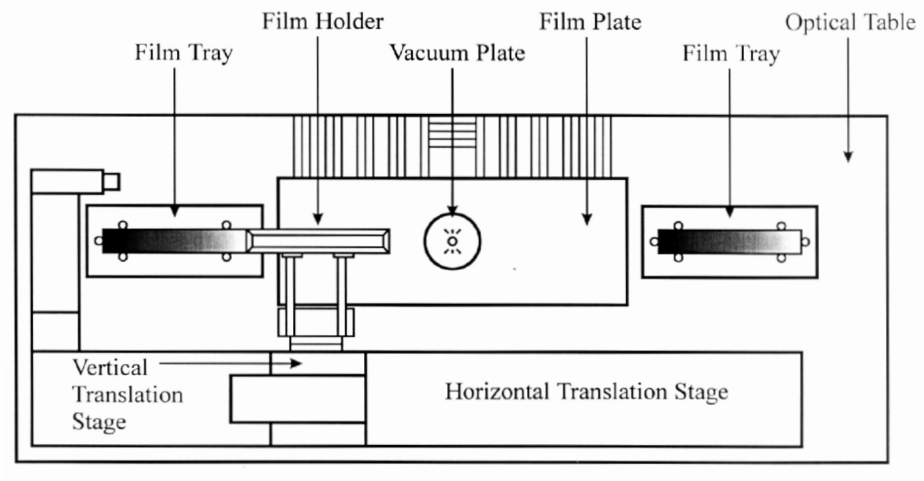

Figure 3. Top view of the film transport system of the visual diffuse transmission densitometer.

diameter of 10 mm at the plane of the opal, which is large enough to capture the entire area from where flux exits a step.

The films of a batch to be measured are loaded into the film holder. For each film, the holder is moved on top of it and the vacuum is applied, attaching the film to the holder. While the steps of the film are centered in their longitudinal direction (parallel to the short dimension of the film) by the position of the holder perpendicular to its horizontal direction of travel, centering the steps in their transverse direction is accomplished by optical means. The location of the boundary between the first and second steps is found by measuring the signal as the film is moved horizontally just above the opal; a 5% decrease in the signal indicates the boundary. The positions of the centers of the steps are then referenced from the location of the boundary.

The film is moved away from the opal and the aperture signal N_j is measured at an amplifier gain $G_j = 10^5$ V/A. The transmitted signal N_τ is measured by moving the film horizontally to center the step on the opal, lowering the film until it is on top of the opal, and applying a vacuum to the vacuum plate while releasing the vacuum on the film holder. The amplifier gain G_τ is selected to yield a signal between 1 V and 12 V. After the last step is measured, the film is moved over the other film tray, the vacuum on the holder is released and air is introduced into the line, and the film falls onto the tray. The aperture signal is measured again as described previously. Dark signals are measured at each amplifier gain with the shutter closed, and these are subtracted from the signals obtained at that gain to yield net aperture and transmitted signals. The two aperture signals are averaged, and Eq. 27 is used to calculate the transmission density of each step, assuming that the photometric responsivity of the detector was constant for all the measurements. Note that only the amplifier gain ratio, G_τ/G_j, is needed for Eq. 27, not the absolute values of the gains.

A batch of films is measured on three separate occasions, and the average transmission density of each step is reported on the calibration certificate that accompanies each film step tablet SRM. The standard deviation of the transmission density must be less than the expanded uncertainty due to random effects detailed below. Proper operation of the densitometer is verified by including in each batch several check standard films that were measured previously.

Densitometer Characterization and Uncertainties

The densitometer was thoroughly characterized, not only to ensure proper operation, but also to verify compliance with the applicable documentary standards for measuring visual diffuse transmission density.[2–4] These standards specify both the geometrical and spectral conditions for this measurement. The characterization also determines the uncertainties in the measurements, that are analyzed following the guidelines given in Ref. 7.

In general, the purpose of a measurement is to determine the value of a measurand y. This result may be obtained from n other quantities x_i through the functional relationship f, given by

$$y = f(x_1, x_2, \ldots, x_i, \ldots, x_n). \tag{30}$$

The standard uncertainty of an input quantity x_i is the estimated standard deviation associated with this quantity and is denoted by $u(x_i)$. The relative standard uncertainty is given by $u(x_i)/x_i$. The standard uncertainties may be classified either by the effect of their source or by their method of evaluation. The effects are either random or systematic; the random effect arising from stochastic temporal or spatial variations in the measurement, and the systematic effect from recognized effects on a measurement. The method of evaluation is either Type A, which is based on statistical analysis, or Type B, which is based on other means.

To first order, the estimated standard uncertainty $u(y)$ in the measurand, due to a standard uncertainty $u(x_i)$ is

$$u(y) = \frac{\partial f}{\partial x_i} \cdot u(x_i), \tag{31}$$

where $\partial f/\partial x_i$ is the sensitivity coefficient. The combined standard uncertainty $u_c(y)$ in the measurand is the root-sum-square of the standard uncertainties associated with each quantity x_i, assuming that these standard uncertainties are uncorrelated. The expanded uncertainty U is given by $k \cdot u_c(y)$, where k is the coverage factor and is chosen on the basis of the desired level of confidence to be associated with the interval defined by U.

The components of uncertainty are conveniently divided into those arising from the operation of the densitometer, compliance with the standards, and the properties of the densitometer and the films. In the first case, the appropriate form of the measurement equation is Eq. 27. Expressing Eq. 27 as

$$D_T = \log_{10}(x) \tag{32}$$

where D_T is the transmission density and x can be a signal or the gain ratio, the sensitivity coefficient is

$$\frac{\partial D_T}{\partial x} = 0.434 \cdot \frac{1}{x}. \tag{33}$$

Therefore, the standard uncertainty $u(D_T)$ due to the standard uncertainty $u(x)$ is

$$u(D_T) = 0.434 \cdot \frac{u(x)}{x}. \tag{34}$$

Note that the standard uncertainty of D_T is proportional to the relative standard uncertainty of x.

There are several components of uncertainty associated with operation of the densitometer and calculating transmission density from Eq. 27. These components are the accuracy of the digital voltmeter, signal noise, lamp stability, detector linearity, and the ratio of the gains.

The uncertainty arising from the accuracy of the digital voltmeter is a systematic effect with a Type B evaluation. Using the manufacturer's specifications, the relative standard uncertainty of N_j is $23 \cdot 10^{-6}$, while the maximum relative standard uncertainty of N_τ is $77 \cdot 10^{-6}$. The combined relative standard uncertainty of the ratio N_j/N_τ is therefore $80 \cdot 10^{-6}$ which, by using Eq. 34, results in a standard uncertainty $u(D_T) << 0.001$. Signal noise and lamp stability result in uncertainties from random effects with Type A evaluations. A typical relative standard deviation of the signal is 0.002, which results in a standard uncertainty $u(D_T) = 0.001$. Likewise, a typical relative standard deviation of the signal from the aper-

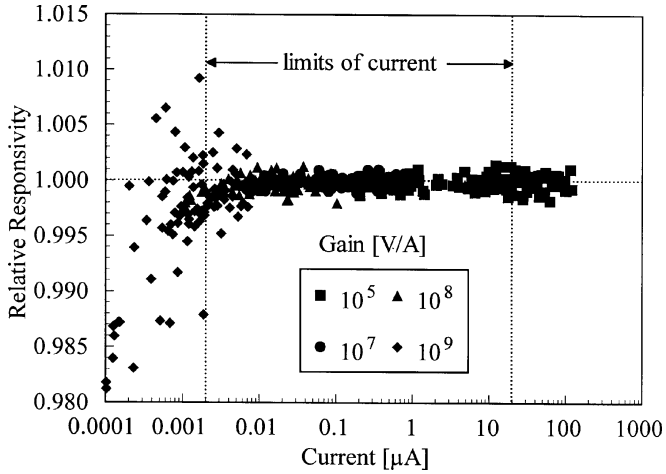

Figure 4. Relative responsivity (measured signal divided by actual flux) of the photodiode and amplifier as a function of current at the amplifier gains given in the legend. The horizontal dotted line indicates the ideal value. Typical limits of the current measured by the densitometer are also indicated.

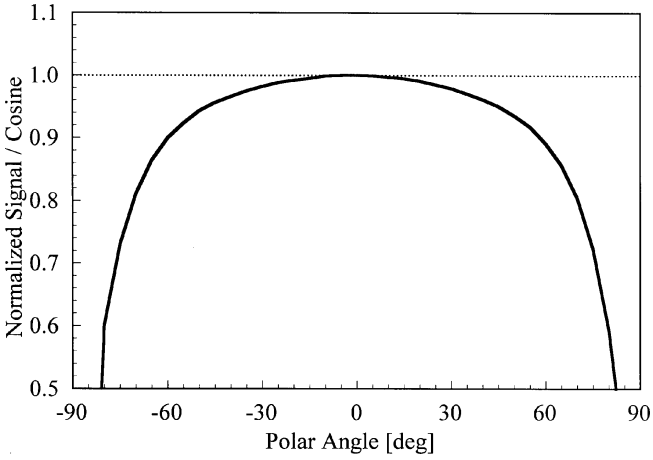

Figure 5. Normalized signal of the efflux from the opal, divided by the cosine of the angle as a function of polar angle. The dotted line indicates the values for a Lambertian diffuser.

ture flux over the time required to measure a film is 0.002.

The linearity of the photodiode-amplifier combination was measured using the beam addition method.[8] The relative responsivity, defined as the ratio of the measured signal to the incident flux, was determined at several amplifier gains and is shown in Fig. 4 as a function of current from the photodiode. Also shown are typical maximum and minimum measured currents. The relative responsivity is close to the ideal value of one over the entire range of measured currents. The uncertainty arising from the detector linearity is a systematic effect with a Type A evaluation. The maximum relative standard deviation of the relative responsivity is 0.0028 at a gain of 10^9 V/A, resulting in a standard uncertainty $u(D_T) = 0.001$.

The gain ratios for successive gains were determined by measuring the voltage output of the amplifier at both gains with the same input current. Combinations of these ratios were then used to calculate the ratio of each gain to the gain of 10^5 V/A. These calculated gain ratios that are not exactly powers of ten, are used in Eq. 27. The uncertainty arising from the gain ratio is a systematic effect with a Type A evaluation. The maximum standard uncertainty in the gain ratios is 10^{-4}, resulting in a standard uncertainty $u(D_T) << 0.001$.

In general, the densitometer complies very well with the documentary standards, and in those instances where it does not, the resulting uncertainties are small. The transmission density of each step is supposed to be measured at its center.[3] However, if the transmission density of a step is not uniform, an uncertainty in centering the step on the opal, arising from random effects with a Type B evaluation, results in an uncertainty in the measured transmission density. The standard uncertainty in centering the step in its transverse direction is 0.5 mm, while in the longitudinal direction the standard uncertainty is 1 mm. From measurements on five representative films of each type, the transmission density varies by much less than 0.001 within 0.5 mm of the center in the transverse direction of the step, and by approximately 0.001 within 1 mm of the center in the longitudinal direction. Therefore, the standard uncertainty $u(D_T)$ due to the uniformity of the steps is 0.001.

Several other geometrical conditions are specified in Ref. 3 and are met with the densitometer. The deviations of the radiance from the opal over its area must be less than 10%; the actual deviations are less than 8%. The half-angle of the acceptance cone must be less than 10°; the half-angle of the densitometer is 9.5°. The step must be in contact with the opal; the vacuum system pulls the step down onto the opal.

The final geometrical condition specified in Ref. 3 is the diffusion coefficient d of the source system that must be greater than or equal to 0.90. The efflux from the source system was measured as a function of polar angle θ using the bi-directional reflectance goniometer of the Spectral Tri-function Automated Reference Reflectometer facility.[9] The normalized signal, divided by $\cos\theta$, as a function of polar angle is shown in Fig. 5. For a Lambertian diffuser, the normalized signal is 1 at all angles, so the decrease of this ratio as the angle changes from 0° indicates that the opal is not Lambertian. The diffusion coefficient is defined using a modification of Eq. 22 for the case of azimuthal symmetry,[3,10] namely

$$d = \frac{\sum (N_j(\theta)/N_j(0)) \cdot \sin\theta}{\sum \cos\theta \cdot \sin\theta} \tag{35}$$

where $N_j(\theta)$ is the signal as a function of polar angle and the summation is over all the angles where the signal was measured. Using Eq. 35, the diffusion coefficient $d = 0.91$ conforms to the standard.

The uncertainty in D_T due to the diffusion coefficient, a systematic effect with a Type B evaluation, is a result of non-ideal hemispherical illumination of the step, and is given by the geometrical correction factor C_g appearing in Eq. 28. However, there is no uncertainty in D_T due to the diffusion coefficient for the SRM film step tablets. The outline of the opal remains sharp even when viewed through steps with the largest transmission densities. Therefore, the steps do not appreciably scatter the incident light and the condition leading to Eq. 20 applies, with the result that $C_g = 1$ and there is no correction from Eq. 28. If the sample is a Lambertian diffuser, then $C_g = 1.0989$ and, from Eq. 28 the measured D_T is greater than the actual D_T by $\log_{10}(C_g) = 0.041$.

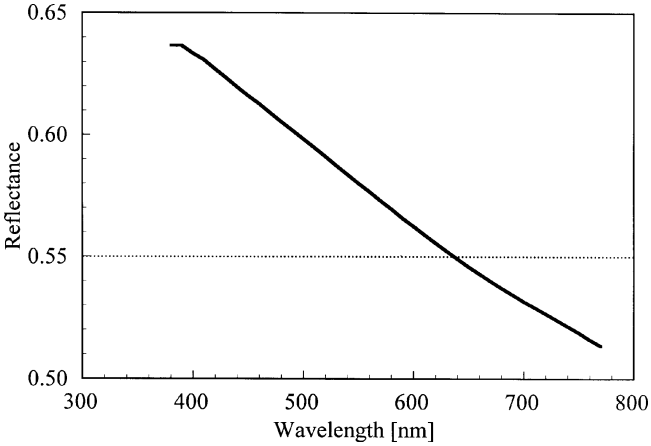

Figure 6. 6°/hemispherical reflectance of the opal as a function of wavelength. The dotted line indicates the value specified in the documentary standard.

The final properties to consider are spectral, which result in uncertainties in D_T from Eq. 28 through the spectral correction factor C_s. The spectral reflectance of the opal $\rho_o(\lambda)$ is specified[4] to be 0.55 ± 0.05. The 6°/hemispherical reflectance of flash opals of the same type used in the densitometer was measured in the Spectral Trifunction Automated Reference Reflectometer facility,[9] and is shown in Fig. 6 as a function of wavelength. The spectral reflectance decreases monotonically with wavelength and is within the values specified by the standard for wavelengths longer than 490 nm.

The spectral flux distribution of the source, $S_H(\lambda)$, is also specified in Ref. 4. This distribution depends upon the opal, infrared filter, and current through the lamp. With the type of opal, lamp, and filter fixed, as well as the thickness of the filter, the only adjustable parameter is the current. Therefore, the optimal current to achieve a close approximation of $S_H(\lambda)$ was determined experimentally using the spectroradiometer in the Low-Level Radiance facility.[11] The best agreement between $S_H(\lambda)$ and the measured spectral flux distribution $S(\lambda)$ was obtained with a lamp current of 7.8 A. The two distributions, normalized at 560 nm, are shown as a function of wavelength in Fig. 7(a). The spectral flux distribution $S(\lambda)$ was relatively insensitive to changes in lamp current of 0.1 A. Because the lamp power supply maintains a constant current to within 1 mA, this distribution is not expected to change during measurements.

The relative spectral response function of the detector system, $V_T(\lambda)$, is specified in Ref. 4 to satisfy Eq. 4. The spectral responsivity of the photodiode was measured in the Spectral Comparator facility,[12] while the spectral transmittance of the photopic filter was measured in the Regular Spectral Transmittance facility.[13] The relative spectral response function $V(\lambda)$ of the densitometer, from the product of the responsivity and transmittance, is shown as a function of wavelength in Fig. 7(b), as well as $V_T(\lambda)$. The relative spectral response function closely approximates $V_\lambda(\lambda)$. Because $V_\lambda(\lambda)$ is widely used, and because no filter could be readily found to correctly modify the relative spectral response function, no attempt was made to obtain $V_T(\lambda)$. The spectral product of the normalized spectral flux distribution and the relative spectral response function, $S(\lambda)\cdot V(\lambda)$, is shown in Fig. 7(c) as a function of wavelength, as well as the specified product $S_H(\lambda)\cdot V_T(\lambda)$.

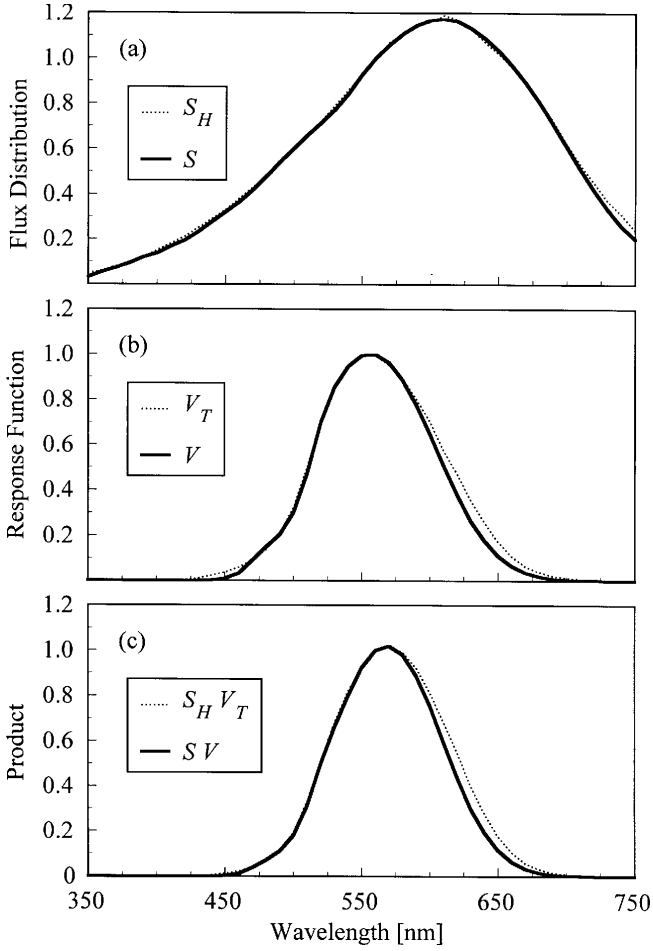

Figure 7. Normalized spectral flux distribution (a), relative spectral response function (b), and spectral product (c) as a function of wavelength. The dashed lines are the values specified by the documentary standards, and the solid lines are the values measured for the densitometer.

To calculate the spectral correction factor from Eq. 16 and the transmittance correction factor from Eq. 24, the spectral transmittance and reflectance of the steps must be known to calculate the spectral hemispherical/directional transmittance factor from Eq. 10. These properties were measured using a commercial spectrophotometer for both types of film step tablets in unexposed areas and are representative of the base films. The spectral directional/hemispherical reflectance and spectral regular transmittance for both types of films are shown in Fig. 8 as a function of wavelength. There is spectral structure in these properties for the x-ray film, giving it a blue tint, while the neutral photographic film has no such spectral structure. The spectral transmittance will, of course, vary between steps, although its spectral shape is expected to remain similar for all steps of the same type of film. The spectral reflectance, on the other hand, should remain the same for all steps of a given film type. Therefore, while the correction factors are calculated using the properties of the base films, there is a possibility of some dependence of these factors on the transmission density of the step.

The spectral correction factor given by Eq. 16 uses the actual values for both the opal spectral reflectance and spectral product, and compares them with the ideal

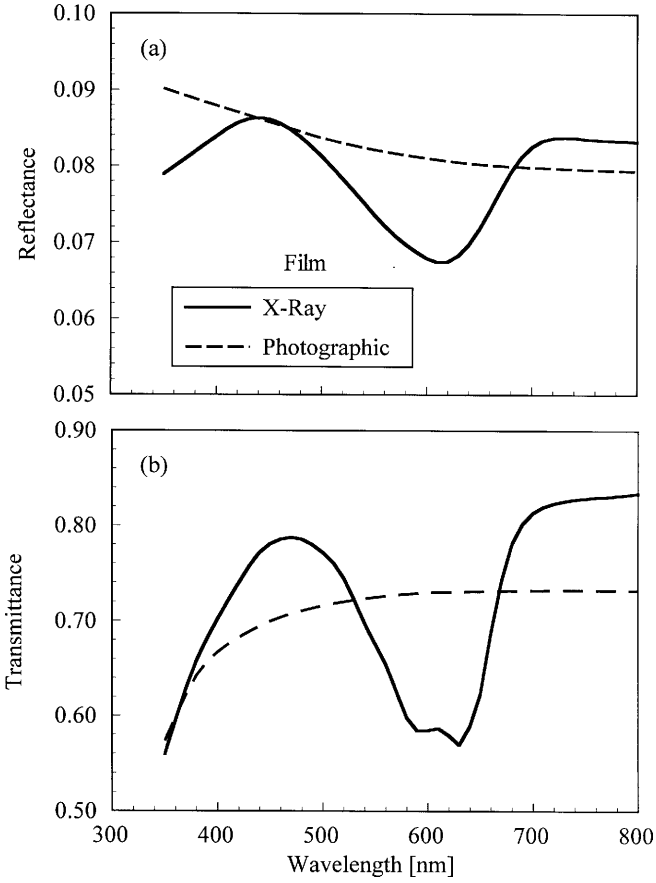

Figure 8. Directional/hemispherical reflectance (a) and regular transmittance (b) of the indicated step tablet film types as functions of wavelength.

values. For this case, the spectral correction factor C_s = 0.9991 and 0.9984 for the x-ray and photographic films, respectively, yielding $\log_{10}(C_s)$ = –0.0004 and –0.0007. Because this correction in Eq. 28 is so small, it is considered as an uncertainty. Furthermore, it is useful to separately calculate spectral correction factors for the opal spectral reflectance and for the spectral product. Assuming an ideal spectral product for the densitometer, the spectral correction factor for the opal $C_{s,o}$ is given by

$$C_{S,O} = \frac{\int d\lambda\, S_A(\lambda)\cdot T_O(\lambda)\cdot V_\lambda(\lambda)}{\int d\lambda\, S_A(\lambda)\cdot T(\lambda)\cdot V_\lambda(\lambda)}, \qquad (36)$$

while for an ideal opal spectral reflectance the spectral correction factor for the spectral product $C_{s,sp}$ is given by

$$C_{s,sp} = \frac{\int d\lambda\, S_A(\lambda)\cdot T_O(\lambda)\cdot V_\lambda(\lambda)}{\int d\lambda\, S_A(\lambda)\cdot T_O(\lambda)\cdot V(\lambda)} \cdot \frac{\int d\lambda\, S(\lambda)\cdot V(\lambda)}{\int d\lambda\, S_A(\lambda)\cdot V_\lambda(\lambda)}. \qquad (37)$$

For the x-ray and photographic films these spectral correction factors are $C_{s,o}$ = 0.9982 and 0.9981 and $C_{s,sp}$ = 1.0010 and 1.0003, respectively, yielding $\log_{10}(C_{s,o})$ = –0.0008 and –0.0008 and $\log_{10}(C_{s,sp})$ = 0.0004 and 0.0001. The small value of 0.0001 for $\log_{10}(C_{s,sp})$ for the photographic film is expected, because the spectral reflectance and transmittance of this film are relatively constant

TABLE I. Components of Uncertainty and the Resulting Standard Uncertainties in Visual Diffuse Transmission Density.

			Standard Uncertainty $u(D_T)$	
Component of Uncertainty	Effect[a]	Type[b]	X-Ray Film	Photographic Film
Voltmeter Accuracy	S	B	<< 0.001	<< 0.001
Signal Noise	R	A	0.001	0.001
Lamp Stability	R	A	0.001	0.001
Detector Linearity	S	A	0.001	0.001
Gain Ratio	S	A	<< 0.001	<< 0.001
Step Uniformity	R	A	0.001	0.001
Diffusion Coefficient	S	B	< 0.001	< 0.001
Opal Reflectance	S	B	0.001	0.001
Spectral Product	S	B	< 0.001	< 0.001
Combined Uncertainty $u_c(D_T)$			0.002	0.002
Expanded Uncertainty U (k = 3)			0.006	0.006

[a] R = random, S = systematic

[b] A = Type A evaluation, B = Type B evaluation

over the wavelength range where the spectral product is appreciable. Considering the various spectral correction factors, the standard uncertainty due to the opal spectral reflectance is assigned to be $u(D_T)$ = 0.001 for both types of films while for the spectral product $u(D_T)$ < 0.001.

The standard uncertainty $u(D_T)$ resulting from each component of uncertainty is given in Table I, along with the combined and expanded uncertainties for each type of film step tablet. A coverage factor k = 3, that defines an interval having a level of confidence of approximately 99.73%, is used for the expanded uncertainty. While a coverage factor k = 2 is customary,[7] the larger coverage factor maintains consistency with previous SRMs of these types and is accepted by users because of the use of the SRMs in the areas of health and safety. From Table I, the components of uncertainty from random effects that contribute significantly to the combined uncertainty are the signal noise, lamp stability, and step uniformity. The expanded uncertainty from the random effects is 0.005. Therefore, as mentioned above, the standard deviation of the three determinations of the transmission density of a step must be less than 0.005 to accept the average as the reported transmission density. Otherwise, the densitometer is assumed to have malfunctioned in some manner during one of the runs and the film is measured again.

The diffusion coefficient of the source system is not a significant source of uncertainty because the steps do not appreciably scatter the influx. For the spectral conditions, even though the opal spectral reflectance and the spectral product do not comply with those specified in the documentary standards, the resulting standard uncertainty in transmission density is only 0.001 in the first case and negligibly small in the second case. Note that these results apply only to the types of films considered in this paper because they depend on the properties of these films, while other films may have different uncertainties.

Finally, while transmission density is measured with the step in contact with an opal, transmittance density would be measured when there is no opal, which is the case for a correct determination of the hemispherical/directional transmittance of a step. The two densities are related by Eq. 29, with the transmittance correction factor C_t given by Eq. 24. For the x-ray films, C_t = 0.9583, while for the photographic films C_t = 0.9532,

yielding $\log_{10}(C_t) = -0.018$ and -0.021, respectively, which, from Eq. 10 are independent of transmission density if the reflectance of the film is likewise independent. Therefore, the transmittance density is always greater than the transmission density because it does not include the effects of inter-reflections between the opal and the step.

Comparisons with other instruments that measure transmission density by an absolute method (without relying upon calibrated standards) are important for verifying the performance of the densitometer described here. While few such densitometers exist, several comparisons have been performed due to the new NIST instrument becoming operational, and are described in detail elsewhere. Briefly, a round-robin comparison among laboratories in the United States resulted in differences in transmission density[14] of less than 0.04, while a comparison with the Physikalisch–Technische Bundesanstalt, the national metrology institute of Germany, found systematic differences[15] of less than 0.015. This later comparison is particularly significant because it demonstrates good agreement between national metrology institutes, although the differences in transmission density are slightly greater than the combined expanded uncertainty for the comparison.

Conclusions

A densitometer is operational at NIST for measuring the visual diffuse transmission density of both x-ray and photographic film step tablet Standard Reference Materials using the diffuse influx mode. It is fully automated so that many films can be measured in one batch run. Comprehensive characterizations of the densitometer were performed to ensure that it complies with the relevant documentary standards for these measurements with the result that the expanded uncertainty ($k = 3$) for visual diffuse transmission density is 0.006.

Acknowledgments. Design, construction, and characterization of the densitometer benefited from discussions with Michael R. Goodwin and Philip Wychorski of the Eastman Kodak Co.

References

1. E. A. Early, T. R. O'Brian, R. D. Saunders, and A. C. Parr, Standard Reference Materials: Film Step Tablet Standards of Diffuse Visual Transmission Density – SRM 1001 and SRM 1008, *Natl. Inst. Stand. Technol., Spec. Publ.* 260–135 (1998).
2. ISO 5–1: Photography – Density Measurements – Part 1: Terms, Symbols, and Notations (1984).
3. ISO 5–2: Photography – Density Measurements – Part 2: Geometric Conditions for Transmission Density (1991).
4. ISO 5–3: Photography – Density Measurements – Part 3: Spectral Conditions (1995).
5. C. S. McCamy, Concepts, Terminology, and Notation for Optical Modulation, *Photogr. Sci. Eng.* **10,** 314 (1966).
6. H. Helmholtz, *Handbuch der Physiologischen Optik*, Leoplold Voss, Leipzig, 1867, p. 168.
7. B. N. Taylor and C. E. Kuyatt, Guidelines for Evaluating and Expressing the Uncertainty of NIST Measurement Results, *Natl. Inst. Stand. Technol. Tech. Note* 1297 (1994).
8. A. Thompson and H.-M. Chen, Beamcon III, a Linearity Measurement Instrument for Optical Detectors, *J. Res. Natl. Inst. Stand. Technol.* **99,** 751 (1994).
9. P. Y. Barnes, E. A. Early and A. C. Parr, NIST Measurement Services: Spectral Reflectance, *Natl. Inst. Stand. Technol. Spec. Publ.* 250–48 (1998).
10. E. Buhr, D. Hoeshen and D. Bergmann, The Measurement of Diffuse Optical Densities. Part I: The Diffusion Coefficient, *J. Imag. Sci. Technol.* **39,** 453 (1995).
11. J. H. Walker and A. Thompson, Spectral Radiance of a Large-Area Integrating Sphere Source, *J. Res. Natl. Inst. Stand. Technol.* **100,** 37 (1995).
12. T. C. Larason, S. S. Bruce and A. C. Parr, Spectroradiometric Detector Measurements: Parts I and II - Ultraviolet and Visible to Near Infrared Detectors, *Natl. Inst. Stand. Technol., Spec. Publ.* 250–41 (1997).
13. K. L. Eckerle, J. J. Hsia, K. D. Mielenz, and V. R. Weidner, Regular Spectral Transmittance, *Natl. Bur. Stand. (U.S.), Spec. Publ.* 250–6 (1986).
14. E. A. Early and T. R. O'Brian, NIST Transmission Density Instrument, *Analytica Chimica Acta* **380,** 143 (1999).
15. E. Buhr, D. Bergmann, E. A. Early, and T. R. O'Brian, Intercomparison of Visual Diffuse Transmission Density Measurements, (in preparation).